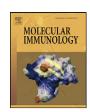
FISHVIED

Contents lists available at ScienceDirect

Molecular Immunology

journal homepage: www.elsevier.com/locate/molimm



Short communication

Structure of the Fab fragment of the anti-murine EGFR antibody 7A7 and exploration of its receptor binding site

Ariel Talavera^{a,b,*,1}, Jenny Mackenzie^{a,1,2}, Greta Garrido^b, Rosmarie Friemann^{a,3}, Alejandro López-Requena^b, Ernesto Moreno^{b,*}, Ute Krengel^{a,**}

- ^a Department of Chemistry, University of Oslo, P.O. Box 1033 Blindern, NO-0315 Oslo, Norway
- ^b Center of Molecular Immunology, P.O. Box 16040, Havana 11600, Cuba

ARTICLE INFO

Article history:
Received 6 December 2010
Received in revised form 28 February 2011
Accepted 17 March 2011
Available online 18 May 2011

Keywords:
Anti-tumor antibody
EGF receptor
High resolution
Immunoglobulin
Murine antibody
X-ray crystal structure

ABSTRACT

The EGF receptor is an important target of cancer immunotherapies. The 7A7 monoclonal antibody has been raised against the murine EGFR, but it cross-reacts with the human receptor. The results from experiments using immune-competent mice can therefore, in principle, be extrapolated to the corresponding scenario in humans. In this work we report the crystal structure of the 7A7 Fab at an effective resolution of 1.4Å. The antibody binding site comprises a deep pocket, located at the interface between the light and heavy chains, with major contributions from CDR loops H1, H2, H3 and L1. Binding experiments show that 7A7 recognizes a site on the EGFR extracellular domain that is not accessible in its most stable conformations, but that becomes exposed upon treatment with a tyrosine kinase inhibitor. This suggests a recognition mechanism similar to that proposed for mAb 806.

© 2011 Elsevier Ltd. All rights reserved.

1. Introduction

The epidermal growth factor (EGF) receptor (EGFR) has become a very attractive target for the treatment of cancer. Its

Abbreviations: CCP4, Collaborative Computational Project, Number 4; CDR, complementarity determining region; CH, heavy chain constant domain; CL, light chain constant domain; EDTA, ethylene diamine tetraacetate; eEGFR, the extracellular domain of the human EGFR; EGF, epidermal growth factor; EGFR, epidermal growth factor receptor; ELISA, enzyme-linked immunosorbent assay; ESFR, European Synchrotron Radiation Facility; Fab, antigen-binding fragment of immunoglobulins; Fc, (1) fragment crystallizable (Fab constant domains), (2) calculated structure factor amplitude; Fo, observed structure factor amplitude; Fv, Fab variable domains; I, intensity; Ig, immunoglobulin; mAb, monoclonal antibody; OD, optical density; PDB, Protein Data Bank; PEG, polyethylene glycol; r.m.s.d., root mean square deviation; VH, variable heavy chain; VL, variable light chain.

overexpression correlates with the development of tumor malignancies, and with poor patient prognosis (Mendelsohn and Baselga, 2006). To inhibit aberrant signaling through the EGFR, two major therapeutic approaches have been devised: the use of small molecules that inhibit the phosphorylation of the intracellular tyrosine kinase domain of the EGFR (Zhang et al., 2007), and the use of monoclonal antibodies that inhibit the receptor activation (Schmitz and Ferguson, 2009).

The anti-EGFR antibodies that are currently in the clinics, *e.g.* Cetuximab (Graham et al., 2004), Panitumumab (Giusti et al., 2007) and Nimotuzumab (Boland and Bebb, 2009), are specific for the human receptor. Therefore, most of the preclinical data for these antibodies are based on human tumor xenograft models in immune-suppressed mice. This has been a drawback since such preclinical models have no capacity to predict the bio-distribution and the activity of these drugs in combination with conventional chemotherapy, radiotherapy or other new agents, or the immune response associated with the therapy (Loisel et al., 2007). An antimurine antibody that exhibits cross-reactivity with the human receptor may be much more favorable in this respect, as it can be studied in its native environment, in immune-competent mice.

Only two antibodies developed against the murine EGFR have been reported to date. One of them is 7A7 (Garrido et al., 2004) and the other one is produced by Imclone (Van Buren et al., 2008; Mutsaers et al., 2009). 7A7 is able to recognize the murine EGFR expressed on normal and tumor cells, as shown by flow

^{*} Corresponding authors at: Center of Molecular Immunology, P.O. Box 16040, Havana 11600, Cuba. Tel.: +53 7 214 3178; fax: +53 7 272 0644.

^{**} Corresponding author at: Department of Chemistry, University of Oslo, P.O. Box 1033 Blindern, NO-0315 Oslo, Norway Tel.: +47 22 85 54 61; fax: +47 22 85 54 41. E-mail addresses: talayera@cim.sld.cu (A. Talayera), emoreno@cim.sld.cu

⁽E. Moreno), ute.krengel@kjemi.uio.no (U. Krengel).

These two authors equally contributed to this work.

² Current address: Axis-Shield PoC AS, P.O. Box 6863 Rodeløkka, NO-0504 Oslo, Norway.

³ Current address: Department of Chemistry, University of Gothenburg, P.O. Box 462, SE-405 30 Gothenburg, Sweden.

cytometry, Western blotting and immunohistochemistry (Garrido et al., 2004). Furthermore, 7A7 inhibits EGF-induced EGFR signaling in D122 tumor cells by reducing EGFR phosphorylation as well as the phosphorylation of molecules involved in downstream EGFR signaling, like ERK, STAT 3 and Akt (Garrido et al., 2007). The antibody has a strong anti-metastatic activity on D122 tumors, for which the contribution of T cells is essential (Garrido et al., 2007). The proposed mechanism for this effect is based on that 7A7 may induce potent cell apoptosis, by the inhibition of EGFR signaling, which causes an "inflammatory microenviroment" leading to the subsequent maturation of dendritic cells (Garrido et al., 2007). In vitro studies indicate that 7A7 displays similar anti-tumor mechanisms as those described for anti-human EGFR mAbs (Garrido et al., 2007). Since 7A7 is also able to react with the human EGFR, it is possible in principle to extrapolate the results from experiments using immune-competent mice to the respective scenario

Here we report the crystal structure of the 7A7 Fab at 1.4 Å resolution, as a first step to characterize its interaction with the EGFR at the molecular level. The structure is compared with the structures of other anti-EGFR antibodies that have been deposited in the Protein Data Bank (PDB) (Berman et al., 2000), all of which are human-specific. Finally, first insights into the 7A7-receptor interaction have been obtained, based on competition studies with the cryoprotectant PEG 400 and with another anti-EGFR antibody.

2. Material and methods

2.1. Fab production and purification

The IgG1 7A7 was produced and purified as previously reported (Garrido et al., 2004). Fab fragments were prepared by 1% papain digestion in 20 mM phosphate buffer, 10 mM cysteine and 10 mM EDTA at 37 °C for 4h. The reaction was stopped by adding iodoacetamide to a final concentration of 20 mM. The 7A7 Fab was purified using a Protein A column, which retains the Fc region. Finally, the protein was concentrated to 12 mg/ml in 25 mM Tris, pH 7.5.

2.2. Crystallization and data collection

Initial crystallization screening was carried out with the Zetasol screen (Molecular Dimentions, Ltd.), using the sitting drop vapor diffusion technique at 20 °C. First crystals appeared after six days, in conditions containing 3.6% PEG 8000 and 0.1 M Tris/Acetate (TrisAc), pH 8.5. To improve the crystals, a grid screen was designed, with PEG concentrations ranging from 3.6% to 15% and the TrisAc pH from 7.0 to 9.5, respectively, followed by additive screening using the Hampton Additive Screen (Hampton Research). Largest crystals were obtained with 15% PEG 8000, 100 mM TrisAc pH 9.0 and 10 mM EDTA. The crystals were cryoprotected by a brief immersion in a reservoir solution supplemented with 10 mM EDTA and 25% PEG 400.

X-ray data were collected in two passes, to 1.3 Å and 3.0 Å resolution, respectively, at beamline ID 14-3 of the European Synchrotron Radiation Facility (ESRF) in Grenoble, France. In each case, 200° of data space were sampled, using oscillation angles of 0.2° and 1.0° for the high and low resolution passes, respectively. The data were processed with iMosflm 0.6.1 (built on the latest Mosflm 7.0.3) (Collaborative Computational Project, Number 4 (CCP4), 1994; Leslie, 2006) and the intensities from the two data sets were thereafter scaled and merged with SCALA (CCP4, 1994; Evans, 2006), cutting the data at 1.4 Å resolution. The crystals had space group C2, with unit cell parameters of a = 169.0 Å, b = 57.3 Å, c = 121.0 Å and $\beta = 102.1^{\circ}$, which suggests a solvent content of 50%, based on its Matthew's coefficient V_M of 2.5 ų/Da (Matthews, 1968;

Table 1Data collection and refinement statistics.

Crystal parameters	
Space group	C2
Unit cell parameters	$a = 169.0 \text{ Å}, b = 57.3 \text{ Å}, c = 121.0 \text{ Å}, \beta = 102.1^{\circ}$
Molecules per asymmetric unit	2
Data-processing statistics	
Resolution range (Å)	23-1.4 (1.48-1.40) ^a
No. of observations	860,418 (114,441)
No. of unique reflections	191,075 (27,729)
Completeness	99.6 (90.0)
$R_{\text{merge}}^{\text{b}}$	0.059 (0.36)
$\langle I/\sigma(I)\rangle$	13.3 (3.2)
Multiplicity	4.5 (4.1)
Refinement statistics	
Resolution (Å)	22.6-1.4
No. of reflections	374,113
$R_{\text{work}}/R_{\text{free}}^{c}$ (%)	14.4/17.6
Number of atoms	
Protein	6868
Ligand	37
Solvent	1116
R.m.s. deviations from ideal geometry ^d	
Bond lengths (Å)	0.008
Bond angles (°)	1.2
Average B factors (Å ²)	
Protein	20
PEG fragments	34
Solvent	36
From Wilson plot	15.5
Ramachandran plote (%)	
In preferred regions	97.5
In allowed regions	2.4
Outliers	0.1
PDB ID	2XKN

^a Values in parentheses refer to high resolution shell.

Kantardjieff and Rupp, 2003). Data collection statistics are summarized in Table 1.

2.3. Structure determination and refinement

The structure of the 7A7 Fab was solved by molecular replacement with the program Phaser (McCoy, 2007), using the structure of another Fab (PDB ID: 1HIL; Rini et al., 1992) as a search model. A rotation and translation search identified two monomers in the asymmetric unit, related by a non-crystallographic translation, however, structure solution was not straightforward. In order to facilitate structure determination, the data were reindexed in 12, a cell choice that did not exhibit the non-crystallographic translation. The structure of the 7A7 Fab could then easily be solved by molecular replacement.

After one round of rigid body refinement with Refmac5 (Murshudov et al., 1997), the electron density was of sufficient quality to rebuild the missing/differing amino acids using the program COOT (Emsley and Cowtan, 2004). This early model of 7A7 was subsequently used to perform molecular replacement using data indexed in C2, since I2 is a non-standard cell choice that is not implemented in all programs.

The new model was subjected to simulated annealing and iterative cycles of positional and temperature-factor refinement with PHENIX (Adams et al., 2002), followed by manual fitting and rebuilding. Alternative side chain conformations were included where warranted. Atomic refinement was performed using PHENIX (Adams et al., 2002). In the final stages of refinement, anisotropic B-

^b $R_{\text{merge}} = \Sigma_h \; \Sigma_i |I_{hi} - \langle I_h \rangle| / \Sigma_h \; \Sigma_i \; \langle I_h \rangle$ where $\langle I_h \rangle$ is the average intensity over symmetry related measurements.

^c $R_{\text{factor}} = \Sigma ||F_0| - |F_c||/\Sigma ||F_0||$ where F_0 and F_c are the observed and calculated F factors, respectively.

^d r.m.s.d.: root mean square deviation from ideal geometry (Engh and Huber, 1991)

^e According to COOT (Emsley and Cowtan, 2004).

Download English Version:

https://daneshyari.com/en/article/2831248

Download Persian Version:

https://daneshyari.com/article/2831248

<u>Daneshyari.com</u>